

Strong localization of terahertz wave and significant enhancement in electric field achieved in U-shaped resonators with a large aspect ratio

Rong-Rong Lin,¹ Ye-Bin Xu,¹ Hai-Ying Liu,¹ Sheng Lan,^{1,a)} and Achanta Venu Gopal²

¹Laboratory of Nanophotonic Functional Materials and Devices, School of Information and Optoelectronic Science and Engineering, South China Normal University, Guangzhou 510006, China

²Department of Condensed Matter Physics and Material Science, Tata Institute of Fundamental Research, Homi Bhabha Road, Mumbai 400005, India

(Received 19 June 2013; accepted 25 August 2013; published online 17 September 2013)

We investigated the transmission of terahertz (THz) wave through periodically arranged split-rectangle resonators with different aspect ratios by using THz time domain spectroscopy. It was found that a narrow resonant mode with a Q factor as large as ~ 20 could be achieved at a low frequency of ~ 0.22 THz in U-shaped resonators with a large aspect ratio of 9. Numerical simulations based on finite-difference time-domain technique revealed that the electric field of the incident THz wave could be strongly localized on the oscillation edges of the U-shaped resonators, leading to an enhancement factor as large as ~ 105 . © 2013 AIP Publishing LLC. [<http://dx.doi.org/10.1063/1.4820809>]

Terahertz (THz) wave, the electromagnetic radiation with frequencies ranging from 0.1 THz to 10 THz, has received intensive and extensive studies in the last decade due to its potential applications in many fields such as spectroscopy of chemical and biological materials, security check, and wireless communication. A big challenge in this research field is how to concentrate or focus THz wave into a region whose dimension is much smaller than its wavelength. The purpose is to enhance the interaction between THz wave and materials and to improve the spatial resolution of THz imaging. So far, various schemes have been proposed to realize the concentration or localization of THz wave. For example, Maier *et al.* proposed the use of corrugated metal wires for the focusing of THz wave.¹ Zhan *et al.* used parallel-plate waveguides to realize the superfocusing of THz wave.² In recent years, Seo *et al.* investigated the significant enhancement of electric field achieved in metallic nano slits whose widths are several orders of magnitude smaller than the wavelength of THz wave.³

For applications such as THz communication and construction of metamaterials, tunable THz band pass or band stop filters with narrow bandwidths or large quality (Q) factors are highly desirable. As the basic units of metamaterials, split-ring resonators (SRRs) have been the focus of many studies.^{4–6} Much effort has been devoted to optimizing the resonator geometry for high Q factors, for example, mirrored arrangement of asymmetric split-ring resonators (ASRs),⁵ different arrangements of SRRs and ASRs,⁶ the design of asymmetric D-split resonators⁷ and paired U-shaped resonators.⁸ On the other hand, the complementary structures of SRRs, i.e., air grooves with the same geometry perforated in metallic films, were also investigated for band pass filter application in the THz spectral region.^{9,10} In particular, Rockstuhl *et al.* compared the resonant modes in SRRs with those in the complementary structures based on Babinet's principle and explained in detail the physical origin of these

modes.¹¹ Very recently, Bitzer *et al.* measured the near-field distributions of the resonant modes in both SRRs and their complementary structures and demonstrated the applicability of Babinet's principle.¹²

For the extraordinary transmission of electromagnetic wave mediated by the excitation of surface plasmon polaritons (SPPs),¹³ the shape of the air holes plays a dominant role in the extraordinary transmission.¹⁴ Basically, extraordinary transmission may depend on many factors such as the metal on which the array of air holes is made,^{15–19} the geometric shape of the air holes,^{20–24} the period of the air hole array,²⁵ the angle of the air hole array with respect to the polarization of the THz wave,^{26,27} and even the ambient environment surrounding the air hole array.^{28,29} So far, various functional devices have been realized by controlling or engineering these parameters.^{5,8,30,31}

Shape resonance in the transmission of THz wave was investigated by using randomly distributed rectangular air holes with different shapes perforated in a metal film.²⁰ For the THz wave incident normally on the metal film, the waveguide mode (i.e., the half-wavelength mode)^{9,25} of the rectangular hole will be excited if the polarization of the THz wave is perpendicular to the long axis of the rectangular hole. In addition, it was found that the frequency of the lowest order resonant mode is determined by $f = c/2b$, where b is the length of the long axis. Apart from rectangular holes, periodically arranged c -shaped or ε -shaped holes were also investigated.^{9,10} It was found that the frequency of the first resonant mode (or transmission peak), which corresponds to the half-wavelength mode, was determined by the total length of the resonator. When a polarized THz wave is incident normally on a split-rectangle resonator, SPPs are only excited on the edges perpendicular to the polarization of the THz wave. Physically, the THz wave resonant with the resonator will be transformed into SPPs which radiate on the other side of the metallic film. As a result, the excited SPPs will be localized on the edges perpendicular to the polarization which will be referred to as oscillation edges hereafter for convenience. Therefore, it is expected that strong

^{a)} Author to whom correspondence should be addressed. Electronic mail: slan@scnu.edu.cn.

localization of THz wave can be achieved by reducing the oscillation edges while keeping the total length of the resonator unchanged.

In this letter, we investigated experimentally and numerically the transmission properties of periodically arranged complementary split-rectangle resonators with different aspect ratios. It was found that strong localization of THz wave and significant enhancement in electric field could be realized in U-shaped resonators with a large aspect ratio of 9. This enhancement is manifested as large Q factor of more than 20 observed at a low frequency of 0.22 THz and was further confirmed by the numerical simulation of the electric field distributions in the split-rectangle resonators.

The array of periodically arranged split-rectangle resonators was fabricated in a 10- μm -thick stainless steel foil by using femtosecond (fs) laser machining. The sample size was 1 cm \times 1 cm. The width of the air groove (w), which was determined by the laser spot size, was measured to be $\sim 50 \mu\text{m}$. The total length of the resonators was fixed at 1950 μm and the split width at 50 μm . The total length of the resonators was chosen such that the frequency of the strongly localized resonant mode is at about the spectral center of the THz short pulses (~ 0.30 THz). Samples containing arrays of split-rectangle resonators with different aspect ratios were fabricated. The sizes of the corresponding rectangles were designed to be 300 $\mu\text{m} \times 700 \mu\text{m}$, 500 $\mu\text{m} \times 500 \mu\text{m}$, 600 $\mu\text{m} \times 400 \mu\text{m}$, 800 $\mu\text{m} \times 200 \mu\text{m}$, and 900 $\mu\text{m} \times 100 \mu\text{m}$, as shown in Figs. 1(b)–1(f). The periods in the x and y directions (p_x and p_y) were chosen to be 1000 μm for the samples shown in Figs. 1(b)–1(d) and 1200 μm for those shown in Figs. 1(e) and 1(f).

The THz short pulses used in the THz time-domain spectroscopy (THz-TDS)³² measurements were generated by exciting the THz emitter (TERA, Ekapla) with fs pulses delivered by a Ti:sapphire oscillator (Mira 900S, Coherent) whose central wavelength, time duration, and repetition rate are 800 nm, 130 fs, and 76 MHz, respectively. The fs laser light was split into two parts, one for exciting the THz emitter and the other for triggering the THz detector (TERA, Ekapla). In the THz-TDS measurements, we changed the angle between the polarization of the THz wave and the split-rectangle resonators, which is denoted as θ , by rotating the samples in the xy plane. The transmission properties of the samples were also simulated by using the finite-difference time-domain (FDTD) technique with non-uniform grid size and perfectly matched layer boundary condition. In the THz spectral region, the influence of the dielectric permittivities of metals on the transmission behavior is quite small. Therefore, we used the dielectric permittivity of gold, which is described by the Drude model, in the numerical simulation. The parameters in the Drude model were chosen to be $\epsilon_\infty = 1$, $\omega_p = 1.37 \times 10^4$ THz, and $\gamma = 40.7$ THz.³

Basically, the incident THz wave will be localized only on the oscillation edges of a resonator that are perpendicular to the polarization of the THz wave through the excitation of SPPs. For horizontally polarized THz wave with $\theta = 0^\circ$, each resonator has a long oscillation edge and two short oscillation edges whose lengths are denoted as L and l , as depicted in Fig. 1. When we reduce the oscillation edges while maintaining the total length of the resonator, it is expected that

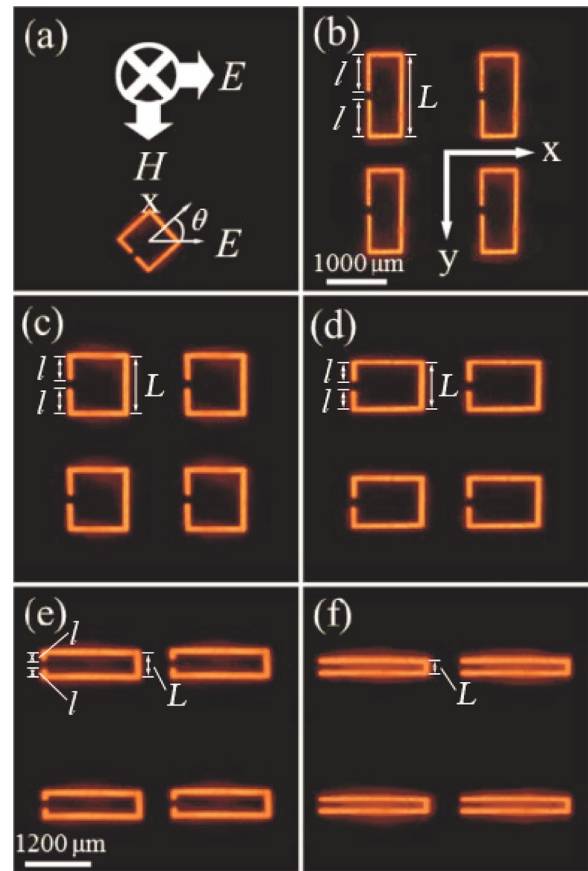


FIG. 1. Microscope images of the samples containing arrays of split-rectangle resonators with different aspect ratios. The sizes of the corresponding rectangles were designed to be: (b) 300 $\mu\text{m} \times 700 \mu\text{m}$, (c) 500 $\mu\text{m} \times 500 \mu\text{m}$, (d) 600 $\mu\text{m} \times 400 \mu\text{m}$, (e) 800 $\mu\text{m} \times 200 \mu\text{m}$, and (f) 900 $\mu\text{m} \times 100 \mu\text{m}$, respectively. The period was chosen to be 1000 μm for the structures shown in (b)–(d) and 1200 μm for those shown in (e) and (f). For horizontally polarized THz wave with $\theta = 0^\circ$, the lengths of the long and short oscillation edges are denoted as L and l , respectively.

the localization of the THz wave will become stronger in the y direction and the quality factor of the resonator will become larger. In order to confirm this idea, we calculated the transmission spectra of all the structures shown in Fig. 1 for the THz wave with a polarization of $\theta = 0^\circ$. The results are shown in Fig. 2(a) where the first two resonant modes are observed at $\nu_1 = 0.072$ and $\nu_2 = 0.22$ THz. They are attributed to the first two odd eigenmodes of the resonator.^{11,12} It is noticed that the resonant mode linewidth narrows with decreasing length of the oscillation edge while the peak position remains nearly unchanged. Meanwhile, the transmission of the resonant modes reduced as the oscillation edge through which the THz wave can transmit the sample has been reduced. It may be noted that the filling ratio of the oscillation edges, which is defined as $[(L + 2l) \times w] / (p_x \times p_y)$, is quite small, especially for the resonator with the shortest oscillation edge of 100 μm ($\sim 0.35\%$), the transmission at the two resonant modes has been greatly enhanced. For $\theta = 90^\circ$, only one resonant mode, which exhibits a similar change with decreasing length of the oscillation edge, is observed at ~ 0.16 THz (not shown). It is the first even eigenmode of the resonator.^{11,12}

In experiments, the transmission spectra of all the samples were characterized by using THz-TDS measurements,

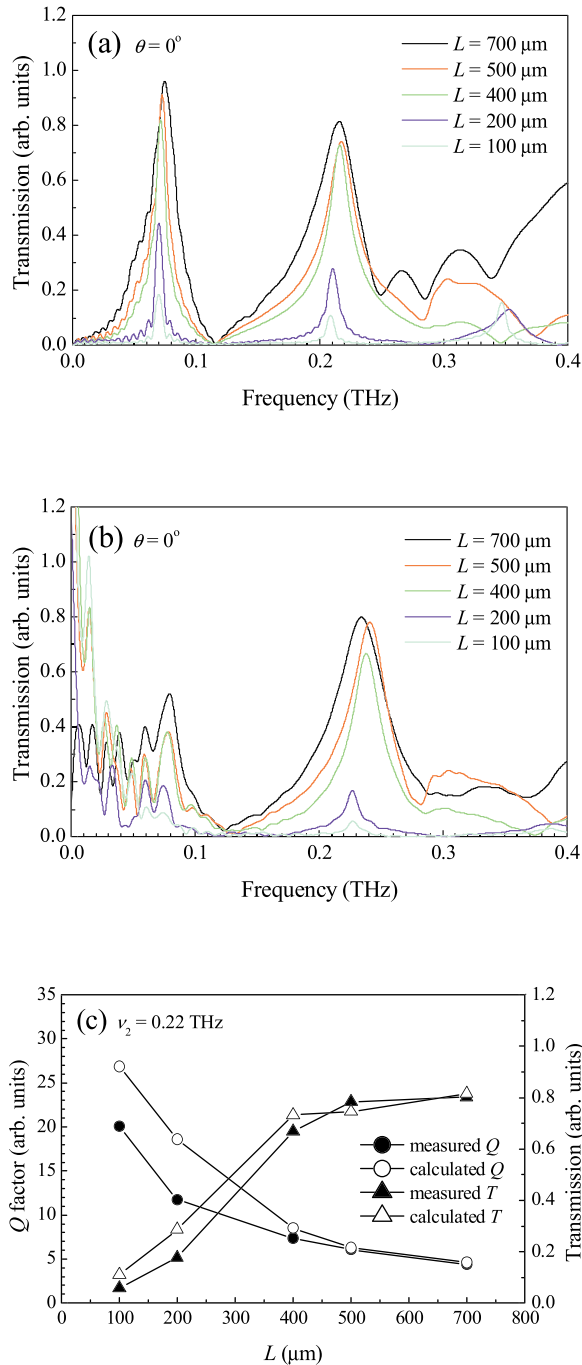


FIG. 2. (a) Calculated transmission spectra for different samples for THz wave with $\theta = 0^\circ$. (b) Measured transmission spectra for different samples for THz wave with $\theta = 0^\circ$. (c) Comparison of the calculated and measured Q factors and transmissions for the resonant mode at $\nu_2 = 0.22$ THz.

and the results for $\theta = 0^\circ$ are presented in Fig. 2(b). The signal to noise ratio of the system for the reference pulse was larger than 280 and the total scan time was 102.4 ps. Since the signal to noise ratio was rather low for frequencies less than 0.1 THz, the resonant mode at $\nu_1 = 0.072$ THz was not clearly resolved. However, the evolution of the resonant mode at $\nu_2 = 0.22$ THz was in good agreement with that predicted by numerical simulation. With decreasing length of the oscillation edges, a narrowing of the linewidth as well as a reduction in transmission was clearly identified. For $\theta = 90^\circ$, very good agreement between the measured and calculated results was also found. The calculated and measured

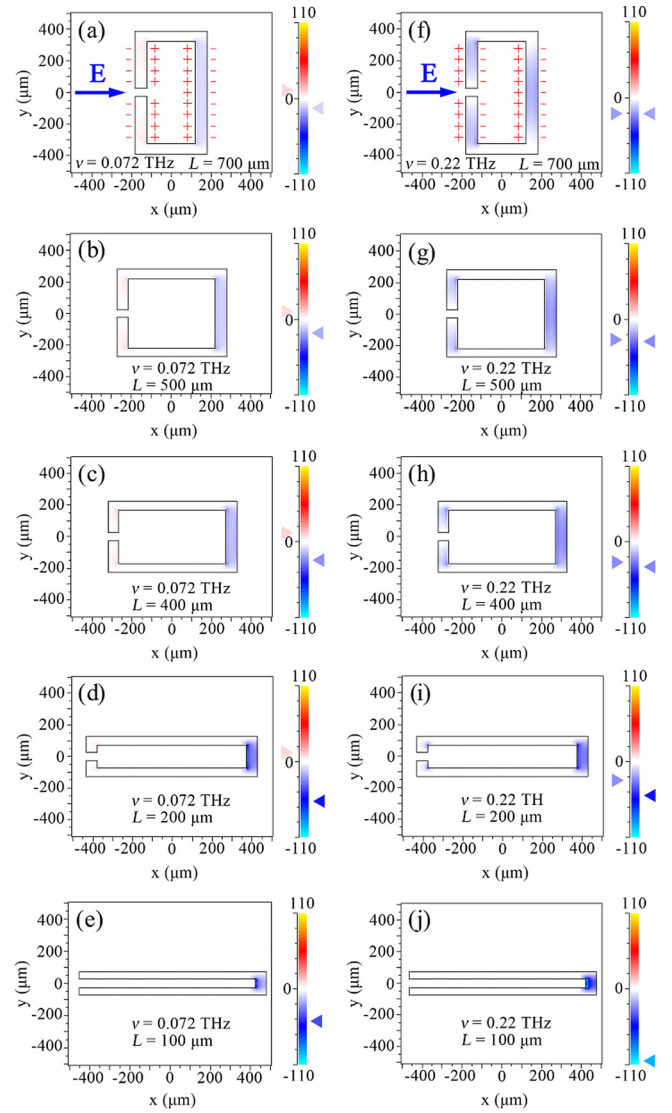


FIG. 3. Calculated electric field distributions on the xy plane ($E_x(x, y)/E_0$) for different resonators at the resonant modes of $\nu_1 = 0.072$ (left panel) and $\nu_2 = 0.22$ THz (right panel). The incident THz wave is polarized along $\theta = 0^\circ$. The amplitude of the electric field has been normalized to that of the incident wave and it gives the enhancement factor in the electric field. The blue and red colors indicate the phase of the electric field and the triangles beside the color bars indicate the maximum enhancement factors.

results described above clearly indicate that the strong localization of the THz wave can be realized by using split-rectangle resonators with a large aspect ratio or short oscillation edges.

In Fig. 2(c), we show the evolution of the Q factor and transmission for the resonant mode at $\nu_2 = 0.22$ THz with decreasing length of the oscillation edge. One can see a dramatic increase in the Q factor and a Q factor as large as ~ 20 achieved in the resonator with the shortest oscillation edge of 100 μm , which is only one-tenth of the central wavelength of the THz wave (~ 1000 μm). In addition, a reduction in the transmission is also observed because of the reduced filling ratio of the oscillation edge.

In order to gain a deep insight into the localization of THz wave on the oscillation edges, the electric field distribution on the xy plane, which is dominated by E_x because $E_y \ll E_x$, was calculated for all the resonators for the THz wave with $\theta = 0^\circ$, as shown in Fig. 3. For the resonator with

$L = 100 \mu\text{m}$, it has only the long oscillation edge (i.e., $l = 0$) and appears to be a U-shaped resonator. In Fig. 3, the left and right panels show the electric field distributions for the resonant modes at $\nu_1 = 0.072 \text{ THz}$ and $\nu_2 = 0.22 \text{ THz}$, respectively. One can see that in both cases the maximum electric field, which appears on the long oscillation edge, increases rapidly with decreasing length of the oscillation edge, indicating the strong localization of the THz wave on the long oscillation edges. It is noticed that the electric fields on the two opposite oscillation edges are out of phase for the resonant mode at $\nu_1 = 0.072 \text{ THz}$ while they are in phase for the resonant mode at $\nu_2 = 0.22 \text{ THz}$, this feature is similar to the result obtained in Ref. 12.

In Fig. 3, it is found that the maximum enhancement in electric field is achieved in the resonator with $L = 200 \mu\text{m}$ for the resonant mode at $\nu_1 = 0.072 \text{ THz}$. In comparison, it is observed in the resonator with $L = 100 \mu\text{m}$ for the resonant mode at $\nu_2 = 0.22 \text{ THz}$. The maximum enhancement factor, which is defined as $E_x(x, y)/E_0$, was calculated to be ~ 70 and ~ 105 for the resonant modes located at 0.072 and 0.22 THz , respectively. It is noticed that the enhancement factor increases with decreasing length of the long oscillation edge. For the resonant mode at $\nu_1 = 0.072 \text{ THz}$, the absence of the two short oscillation edges in the resonator ($L = 100 \mu\text{m}$) leads to a reduction in the enhancement factor. For the resonant mode at $\nu_2 = 0.22 \text{ THz}$, however, a significant enhancement in electric field is observed in the resonator without the two short oscillation edges, i.e., in the U-shaped resonator ($L = 100 \mu\text{m}$ and $l = 0$). This difference can be understood by considering the charge distributions in the resonator for the two resonant modes, as schematically illustrated in Figs. 3(a) and 3(f). Similar charge distributions for the two resonant modes were also demonstrated by THz near-field microscopy.¹² For the resonant mode at $\nu_1 = 0.072 \text{ THz}$, the charge distribution on the oscillation edges is as shown in Fig. 3(a) because of the out of phase electric fields on the long and short oscillation edges (see the left panel of Fig. 3). The positive charges distributed on the right side of the two short air grooves will facilitate the transfer of more negative charges from the left side of the long oscillation edge to the right side of the short oscillation edges, leading to a strong electric field on the long oscillation edge. Therefore, the absence of the short oscillation edges results in a weaker electric field on the long oscillation edge, as can be seen in Fig. 3(e). The situation is completely different when the resonant mode at $\nu_2 = 0.22 \text{ THz}$ is considered as it has in phase electric fields on the long and short oscillation edges (see the right panel of Fig. 3). As shown in Fig. 3(f), the negative charges distributed on the right side of the two short air grooves will hamper the transfer of negative charges from the left side of the long oscillation edge to the right side of the short oscillation edges. As a result, a significant enhancement in the electric field is achieved in the U-shaped resonator without the short oscillation edges, as can be seen in Fig. 3(j). Since the strong localization of electric field requires an oscillation edge with a small length, it is suggested that strong localization of THz wave and significant enhancement in electric field can be realized in U-shaped resonators with a large aspect ratio.

From the simulation and experimental results, it was found that the narrowing of the linewidth was usually

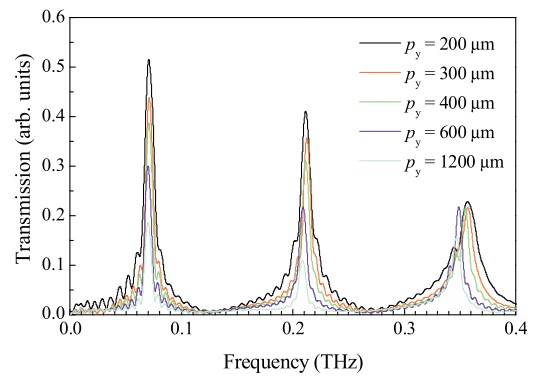


FIG. 4. Calculated transmission spectra are shown for periodic arrays of split-rectangle resonators with different periods in the y direction (p_y).

accompanied by a reduction in the transmission when we reduced the oscillation edges of the resonators. This feature limits the use of such resonators in band pass filters. Basically, the resonant mode is mainly determined by the shape of the resonators and the influence of the period on the transmission is quite small. For split-rectangle resonators with short oscillation edges or a large aspect ratio, the transmission of the resonant mode can be significantly enhanced by reducing the period in the y direction. For the U-shaped resonator with $L = 100 \mu\text{m}$, we simulated transmission spectra for the arrays with different periods of $1200, 600, 400, 300,$ and $200 \mu\text{m}$ in the y direction and the same period in the x direction ($1200 \mu\text{m}$), as shown in Fig. 4. When the period in the y direction is reduced from $1200 \mu\text{m}$ to $200 \mu\text{m}$, the transmission is increased from 0.18 to 0.52 for the resonant mode at $\nu_1 = 0.072 \text{ THz}$ and from 0.11 to 0.41 for the resonant mode at $\nu_2 = 0.22 \text{ THz}$.

In summary, we have investigated experimentally and numerically the localization of THz wave in a deep sub-wavelength region by using periodically arranged split-rectangle resonators with a large aspect ratio or short oscillation edges. A narrow resonant mode with a Q factor as large as ~ 20 was achieved at a low frequency of 0.22 THz in U-shaped resonators with a large aspect ratio of 9 . Very good agreement between the numerical simulation and the experimental observation was obtained. A significant enhancement in the electric field with an enhancement factor more than 100 was achieved on the oscillation edge whose dimension is only one-tenth of the wavelength of the THz wave. In addition, it is revealed that the transmission of the resonant mode can be increased by reducing the period in the direction perpendicular to the polarization of the THz wave. The strong localization of THz wave will significantly enhance the interaction between THz wave and materials. Therefore, the U-shaped resonators with a large aspect ratio proposed in this work may find applications in highly sensitive sensors, narrow band filters, and other optical components in the THz spectral region.

The authors acknowledge the financial support from the National Natural Science Foundation of China (Grant No. 51171066), the Ministry of Education of China (Grant No. 20114407110002), and the project for high-level professionals in the Universities of Guangdong Province, China.

- ¹S. A. Maier, S. R. Andrews, L. Martín-Moreno, and F. J. García-Vidal, *Phys. Rev. Lett.* **97**, 176805 (2006).
- ²H. Zhan, R. Mendis, and D. M. Mittleman, *Opt. Express* **18**, 9643 (2010).
- ³M. A. Seo, H. R. Park, S. M. Koo, D. J. Park, J. H. Kang, O. K. Suwal, S. S. Choi, P. C. M. Planken, G. S. Park, N. K. Park, Q. H. Park, and D. S. Kim, *Nat. Photonics* **3**, 152–156 (2009).
- ⁴W. J. Padilla, A. J. Taylor, C. Highstrete, M. Lee, and R. D. Averitt, *Phys. Rev. Lett.* **96**, 107401 (2006).
- ⁵I. Al-Naib, R. Singh, C. Rockstuhl, F. Lederer, S. Delprat, D. Rocheleau, M. Chaker, T. Ozaki, and R. Morandotti, *Appl. Phys. Lett.* **101**, 071108 (2012).
- ⁶I. Al-Naib, R. Singh, M. Shalaby, T. Ozaki, and R. Morandotti, *IEEE J. Sel. Top. Quantum Electron.* **19**, 8400807 (2013).
- ⁷C. Jansen, I. A. I. Al-Naib, N. Born, and M. Koch, *Appl. Phys. Lett.* **98**, 051109 (2011).
- ⁸Q. Li, X. Zhang, W. Cao, A. Lakhtakia, J. F. O' Hara, J. Han, and W. Zhang, *Appl. Phys. A* **107**, 285–291 (2012).
- ⁹J. W. Lee, M. A. Seo, S. C. Jeoung, Q.-H. Park, and D. S. Kim, *Proc. SPIE* **6351**, 63512B (2006).
- ¹⁰J. W. Lee, M. A. Seo, D. J. Park, and D. S. Kim, *Opt. Express* **14**, 1253 (2006).
- ¹¹C. Rockstuhl, T. Zentgraf, T. P. Meyrath, H. Giessen, and F. Lederer, *Opt. Express* **16**, 2080 (2008).
- ¹²A. Bitzer, A. Ortner, H. Merbold, T. Feurer, and M. Walther, *Opt. Express* **19**, 2537 (2011).
- ¹³X. Fang, Z. Li, Y. Long, H. Wei, R. Liu, J. Ma, M. Kamran, H. Zhao, X. Han, B. Zhao, and X. Qiu, *Phys. Rev. Lett.* **99**, 066805 (2007).
- ¹⁴K. J. K. Koerkamp, S. Enoch, F. B. Segerink, N. F. van Hulst, and L. Kuipers, *Phys. Rev. Lett.* **92**, 183901 (2004).
- ¹⁵J. Pearce and D. M. Mittleman, *Opt. Lett.* **26**, 2002 (2001).
- ¹⁶C.-F. Hsieh and R.-P. Pan, *Opt. Lett.* **31**, 1112 (2006).
- ¹⁷T. H. Isaac, J. Gómez Rivas, and E. Hendry, *Phys. Rev. B* **80**, 193412 (2009).
- ¹⁸H. E. Arabi, M. Park, M. Pournoury, and K. Oh, *Opt. Express* **19**, 8514 (2011).
- ¹⁹B. Scherger, M. Scheller, N. Vieweg, S. T. Cundiff, and M. Koch, *Opt. Express* **19**, 24884 (2011).
- ²⁰J. W. Lee, M. A. Seo, D. H. Kang, K. S. Khim, S. C. Jeoung, and D. S. Kim, *Phys. Rev. Lett.* **99**, 137401 (2007).
- ²¹M. M. J. Treacy, *Phys. Rev. B* **66**, 195105 (2002).
- ²²F. Yang and J. R. Sambles, *Phys. Rev. Lett.* **89**, 063901 (2002).
- ²³J. Han, A. K. Azad, M. Gong, X. Lu, and W. Zhang, *Appl. Phys. Lett.* **91**, 071122 (2007).
- ²⁴D. Qu, D. Grischkowsky, and W. Zhang, *Opt. Lett.* **29**, 896 (2004).
- ²⁵D. Li, G. Li, H. Kong, S. Shu, G. Ma, J. Ge, S. Hu, and N. Dai, *J. Infrared Millim. Terahz Waves* **33**, 212 (2012).
- ²⁶J. Dintinger, S. Klein, F. Bustos, W. L. Barnes, and T. W. Ebbesen, *Phys. Rev. B* **71**, 035424 (2005).
- ²⁷D. Hu and Y. Zhang, *Optik* **121**, 1423 (2010).
- ²⁸Y.-Y. Wang, C.-H. Zhang, J.-L. Ma, B.-B. Jin, W.-W. Xu, L. Kang, J. Chen, and P.-H. Wu, *Acta Physica Sinica* **58**, 6884 (2009).
- ²⁹H. Chen, X.-M. Wu, and W.-X. Yang, *Chin. Phys. Lett.* **27**, 010701 (2010).
- ³⁰S. A. Maier, P. G. Kik, H. A. Atwater, S. Meltzer, E. Harel, B. E. Koel, and A. A. G. Requicha, *Nature Mater.* **2**, 229–232 (2003).
- ³¹S. Das, K. M. Reza, and M. A. Habib, *J. Infrared Millim. Terahz Waves* **33**, 1163 (2012).
- ³²S. Liang, H.-Y. Liu, Q.-F. Dai, L.-J. Wu, S. Lan, and A. V. Gopal, *J. Appl. Phys.* **109**, 024902 (2011).